

Comparison of Cancer-Cell Seeding, Viability and Deformation in the Lung, Muscle and Liver, Visualized by Subcellular Real-time Imaging in the Live Mouse

KATSUHIRO HAYASHI^{1,2,3}, HIROAKI KIMURA^{1,2,3}, KENSUKE YAMAUCHI³, NORIO YAMAMOTO³, HIROYUKI TSUCHIYA³, KATSURO TOMITA³, HIROYUKI KISHIMOTO^{1,2,4}, AKIHIRO HASEGAWA¹, MICHAEL BOUVET² and ROBERT M. HOFFMAN^{1,2}

¹AntiCancer Inc., San Diego, CA, U.S.A.;

²Department of Surgery, University of California, San Diego, CA, U.S.A.;

³Department of Orthopaedic Surgery, School of Medicine, Kanazawa University, Kanazawa, Ishikawa, Japan;

⁴Department of Gastroenterological Surgery, Okayama University Graduate School of Medicine, Dentistry and Pharmaceutical Sciences, Okayama, Japan

Abstract. *The comparison of cancer cell seeding, deformation and viability in the lung, muscle and liver of nude mice in real-time is reported here. The mice were intubated to support ventilation with positive end-respiratory pressure (PEEP) for imaging on the lung. Human fibrosarcoma cells with green fluorescent protein (GFP) in the nucleus and red fluorescent protein (RFP) in the cytoplasm (dual-color HT-1080 cells) were injected into the tail vein for lung imaging, the portal vein for liver imaging or the abdominal aorta for muscle imaging which was performed with an Olympus OV100 Small Animal Imaging System. The length of the cytoplasm and nuclei in 20 seeded cancer cells were measured. A large number of cells initially arrested in the lung capillaries and many cells formed aggregates. The cell number decreased rapidly at 6 and 24 h. There was no significant difference in cancer cell survival when immunocompetent C57BL/6 mice were used in place of the nude mice, suggesting that T cell reaction is not very important in the first 24 h after seeding of cancer cells in the lung. In the lung and liver, little cancer cell deformation occurred. In contrast in the muscle, the cytoplasm and nuclei of the seeded cells were highly deformed and many fragmented cells were observed. The rate of cancer cell death was highest in the lung and lowest in the muscle. In each organ, single disseminated cells tended to die earlier than aggregated cells. The results of this study suggest that the early steps of metastasis are different in the lung, liver and muscle.*

Correspondence to: Robert M. Hoffman, Ph.D., AntiCancer Inc., 7917 Ostrow Street, San Diego, CA 92111, U.S.A. Tel: +1 8586542555, Fax: +1 8582684175, e-mail: all@anticancer.com

Key Words: Green fluorescent protein, red fluorescent protein, cancer cell seeding, real-time imaging, lung, liver, muscle.

Our laboratory pioneered *in vivo* imaging with green fluorescent protein (GFP) and/or red fluorescent protein (RFP). These very bright proteins have made it possible to observe cellular behavior in primary tumors and metastases in live animals (1-3). Dual-color cancer cells, in which GFP is expressed in the nucleus and RFP is expressed in the cytoplasm, were also developed in our laboratory (4) to enable real-time nuclear-cytoplasmic dynamics to be visualized in living cells by subcellular *in vivo* imaging (5, 6).

The mechanism through which circulating tumor cells form metastatic colonies is poorly understood. We previously developed a mouse model to image single cancer-cell dynamics of metastasis to the lung in real-time. By keeping the mice alive, imaging could be repeated to follow the fate of the seeded cancer cells (7).

In the present report, cancer cell seeding, viability and deformation were compared in the lung, liver and muscle by subcellular *in vivo* fluorescence imaging, in mice.

Materials and Methods

Establishment of dual-color cancer cell lines. To establish HT-1080 human fibrosarcoma (HT-1080) (American Type Culture Collection, Manassas, VA, USA) GFP-RFP cells, the cells were transfected with retroviral DsRed2 and H2B-GFP vectors as previously described (4). In brief, the Hind III/Not I fragment from pDsRed2 (Clontech Laboratories Inc., Palo Alto, CA, USA), containing the full-length RFP cDNA, was inserted into the Hind III/Not I site of pLNCX2 (Clontech Laboratories Inc.) containing the neomycin resistance gene. PT67, a NIH3T3-derived packaging cell line (Clontech Laboratories Inc.) expressing the 10 A1 viral envelope (8), was cultured in DMEM (Irvine Scientific, Santa Ana, CA, USA) supplemented with 10% heat-inactivated fetal bovine serum (FBS; Gemini Bio-Products, Calabasas, CA, USA). For vector production, the PT67 cells, at 70% confluence, were incubated with a precipitated mixture of LipofectAMINE reagent (Life Technologies

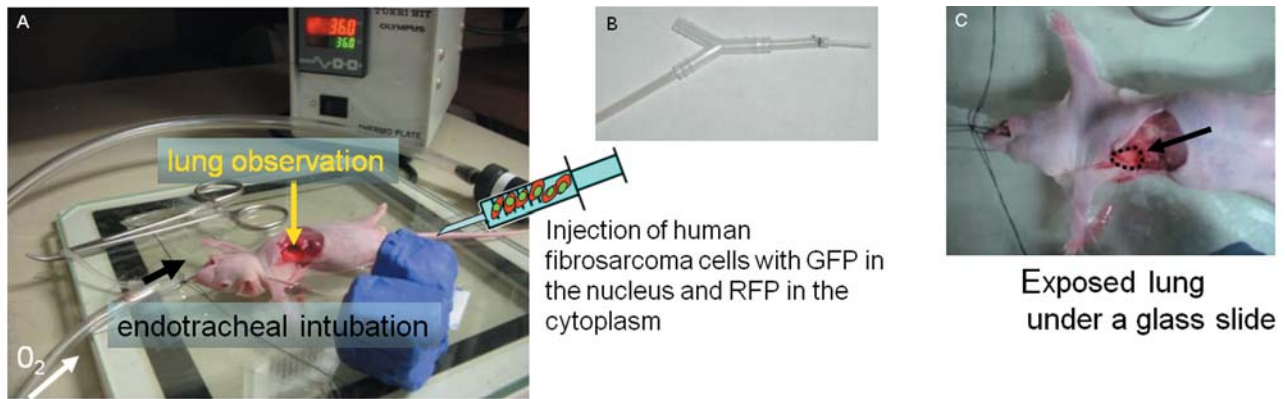


Figure 1. Mouse cancer cell imaging of the lung. A: Nude mouse with oxygen supplied via endotracheal intubation with lung exposed through opened chest wall. Dual colored HT-1080 fibrosarcoma cells were injected into tail vein (7). GFP: green fluorescent protein; RFP: red fluorescent protein. B: Endotracheal intubation tube with a 1.19 mm OD (outer diameter). An exhaust tube was attached to Y-type connector. C: Dotted line shows the exposed right lung lobe under a glass slide.

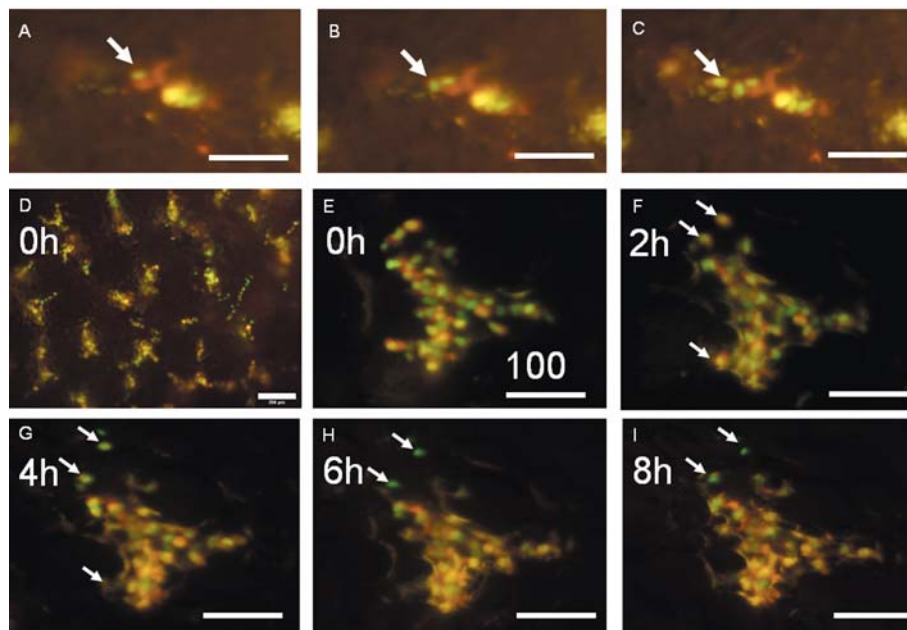


Figure 2. Time course of the lung seeding after injection of human HT-1080 fibrosarcoma cells with GFP in the nucleus and RFP in the cytoplasm. A to C: Time duration: 1 second. Cancer cells arrive and aggregate in the lung capillaries. D: Low magnification at 0 h. Cells arrested in capillaries, forming aggregates. E to I: High magnification. Dying cells can also be seen (arrows). Bars: A-C: 100 μ m; D: 200 μ m; E-I: 100 μ m.

Inc., Grand Island, NY, USA) and saturating quantities of pLNCX2-DsRed2 plasmid for 18 h. Fresh medium was replenished at this time. The cells were examined by fluorescence microscopy 48 h post-transfection. For selection of a clone producing high levels of the RFP retroviral vector (PT67-DsRed2), the cells were cultured in the presence of 200–800 mg/ml G418 (Life Technologies Inc.) increased stepwise over 7 days (4, 8).

The histone H2B gene has no stop codon, thereby enabling the ligation of the H2B gene to the 5'-coding region of the GFP gene

(Clontech Laboratories Inc.). The histone H2B-GFP fusion gene was then inserted at the Hind III/Cal I site of the pLHCX (Clontech Laboratories Inc.) that has the hygromycin resistance gene. To establish a packaging cell clone producing high levels of histone H2B-GFP retroviral vector, the pLHCX histone H2B-GFP plasmid was transfected in PT67 cells using the same methods as described above for PT67-DsRed2. The transfected cells were cultured in the presence of 200–800mg/ml hygromycin (Life Technologies Inc.) increased stepwise over 7 days (4, 8).

For RFP and H2B-GFP gene transduction, 70% confluent HT-1080 cells were used. To establish dual-color cells, clones of these cells expressing RFP in the cytoplasm were initially established. In brief, the cells were incubated with a 1:1 precipitated mixture of retroviral supernatants of PT67-RFP cells and RPMI 1640 (Irvine Scientific) containing 10% FBS for 72 h. Fresh medium was replenished at this time. The cells were harvested with trypsin/EDTA 72 h post-transduction and subcultured at a ratio of 1:15 into selective medium, which contained 200 mg/ml G418. The level of G418 was increased stepwise up to 800 mg/ml (4, 8).

For establishing dual-color cells, the cells were then incubated with a 1:1 precipitated mixture of retroviral supernatants of PT67 H2B-GFP cells and culture medium. To select the double transformants, the cells were incubated with hygromycin 72 h after transfection. The level of hygromycin was increased stepwise from 200 to 800 mg/ml (4, 8).

Proliferation of fluorescent protein-labeled cells in vitro. Dual-color HT-1080 cells were seeded at a density of 1×10^3 cells/dish in 100-mm dishes with RPMI with 10% FBS medium (day 1). The dishes were kept in an incubator at 37°C and 5% CO₂. Every other day (days 2-8), three dishes for each clone were used for cell counting. In brief, resuspended cells collected after trypsinization were stained with trypan blue (Sigma-Aldrich, St. Louis, MO, USA). Only the viable cells were counted with a hemocytometer (Hausser Scientific, Horsham, PA, USA) (4, 8).

Mice. Athymic NCR nude mice (*nu/nu*) and immunocompetent C57BL/6 mice, at 4-6 weeks of age, were used in this study. The breeding pairs were obtained from Charles River Laboratories (Wilmington, MA, USA). The mice were kept in a barrier facility under high-efficiency particulate air (HEPA) filtration and fed with autoclaved laboratory rodent diet. All the animal studies were conducted in accordance with the principals and procedures outlined in the National Research Council's Guide for the Care and Use of Laboratory Animals under assurance number A3873-1 (7).

Mouse endotracheal intubation procedure. We previously developed a novel retrograde wire-guided endotracheal intubation procedure for mice (7): The mice were anesthetized with a ketamine mixture (10 ml ketamine HCL, 7.6 ml xylazine, 2.4 ml acepromazine maleate and 10 ml H₂O) *via* subcutaneous (*s.c.*) injection. The mice were then placed supine on a glass Thermo Plate (Olympus Corp., Tokyo, Japan) in order to maintain constant body temperature throughout the experiment and fixed with plastic tape. A cylindrical column, for example the lid of a needle, was put under the neck to extend the head and neck. An intravenous catheter (SURFLO1, 20 gauge, 25 mm length; Terumo Medical Corporation, Elkton, MD, USA) was used as an endotracheal tube. The catheter had a round molded tip to prevent damage to the soft tissue by sharp edges. This was achieved by briefly placing the tip in an open flame. A 5 mm skin incision was made above the trachea, and then the subcutaneous tissue was separated and the submandibular gland was moved aside to expose the trachea, making it easy to confirm if intubation was successful and not into the esophagus. A small hole (about 1 mm in diameter) was then made in the trachea with a 27-gauge needle (Becton Dickinson and Co., Franklin Lakes, NJ, USA) in order to insert a guide wire (monofilament wire, 0.28 mm in diameter). The endotracheal catheter which was inserted through the mouth and could then be accurately introduced into the trachea over the guide wire. An adequate intubation depth was obtained when the root of the catheter reached the incisors (7).

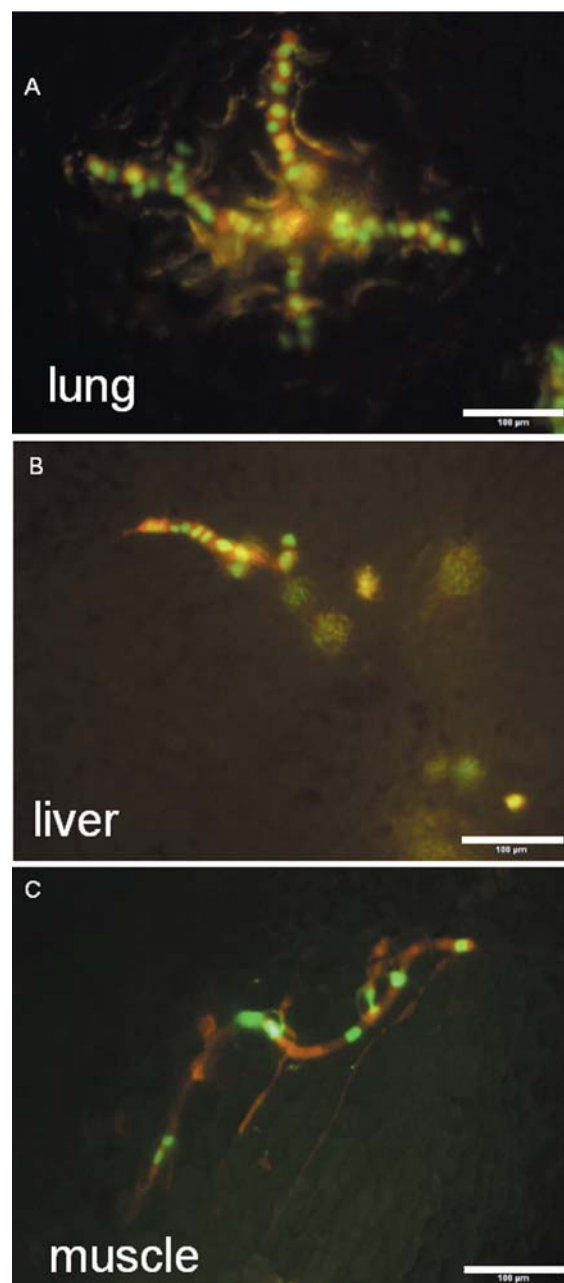


Figure 3. *Cancer cell deformation in lung, liver and muscle.* A: HT-1080 cells in the lung after injection into the tail vein. Little cell deformation was observed. B: HT-1080 cells in the liver after injection into the portal vein. Cell deformation was similar to the lung. C: Highly deformed HT-1080 cells apparent in the muscle after injection into the abdominal aorta. Bars: A-C 100 µm.

According to our previously-developed procedure (7), after endotracheal intubation, the intubation tube was attached and tied to a Y-type connector (3.2 mm OD, Nalgene, Rochester, NY, USA), and a 5-cm exhaust tubing (1.47 mm ID, 1.96 mm OD) was attached to one end of the Y-shape connector. The oxygen tube was

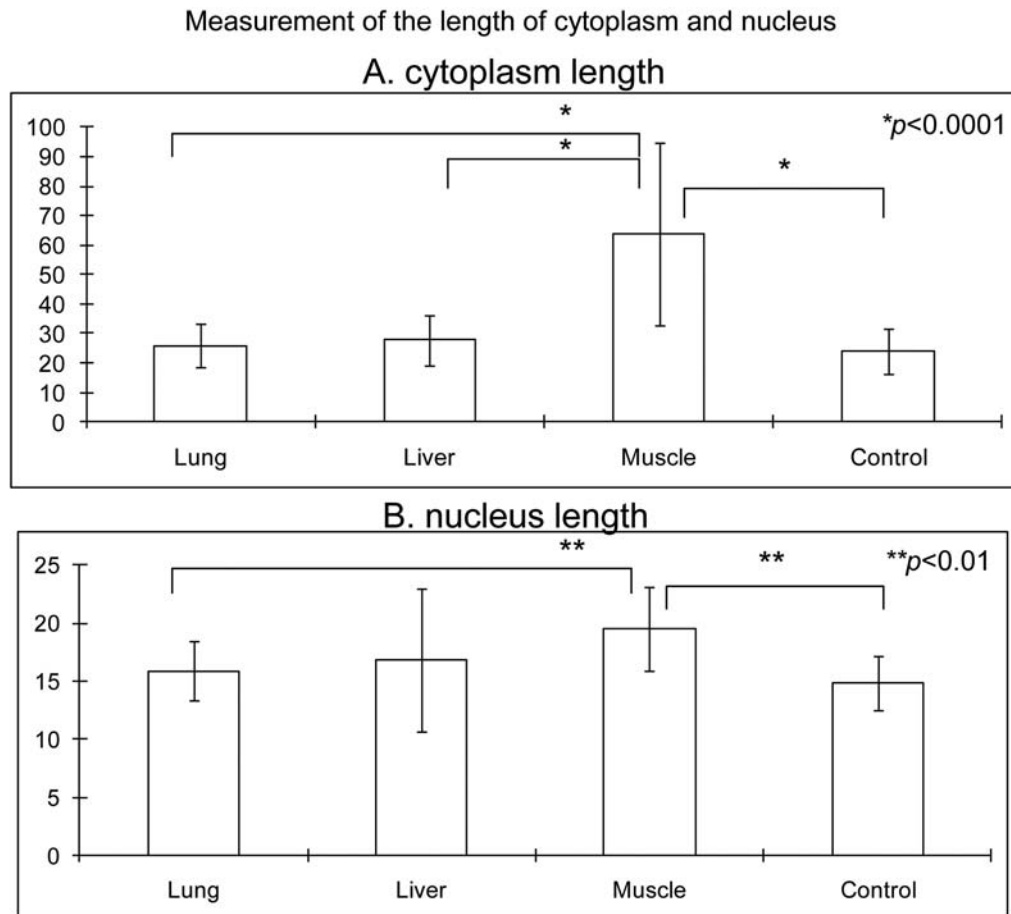
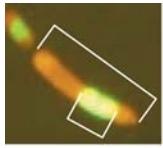


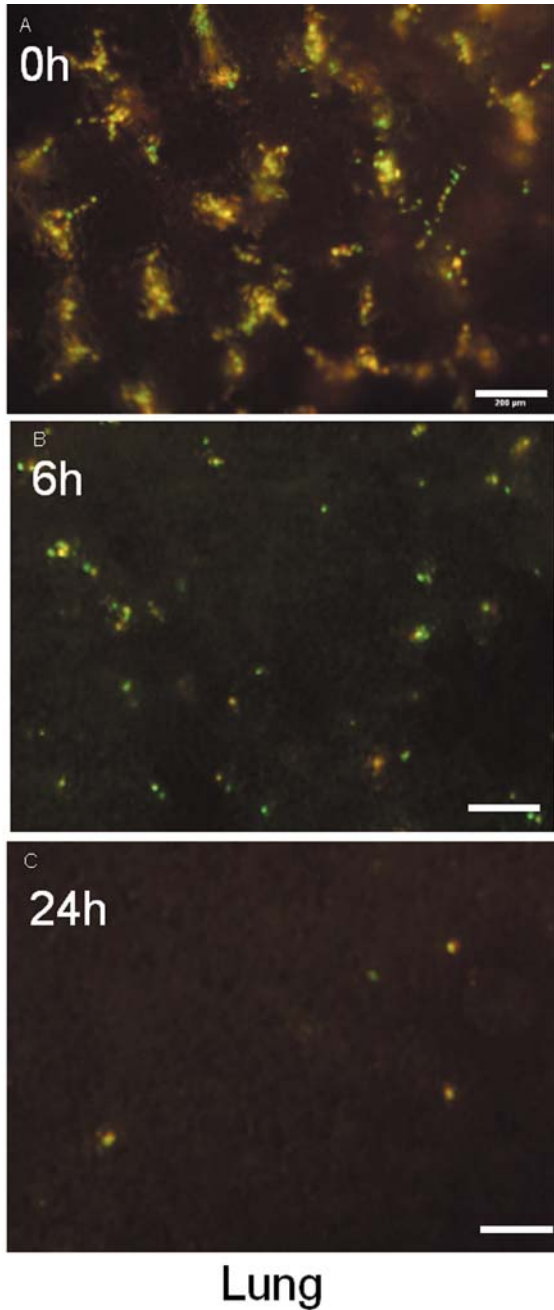
Figure 4. Quantitation of cell deformation in the lung, liver and muscle. Mean length of cytoplasm (A) and nuclei (B) in 20 dual-color HT-1080 cancer cells were measured (5). In the lung and liver, deformation was minimal. In the muscle, the cells were highly deformed. The length of the cytoplasm was significantly different between muscle and liver or lung. The length of the nuclei was significantly different between muscle and lung. Dual color HT1080 cells with GFP expressed in the nucleus and RFP expressed in the cytoplasm. Brackets show how cytoplasm and nuclear lengths were measured.

connected to the Y-shaped connector. At this point, the chest cavity was opened. To maintain anesthesia throughout the procedure, an inhalant anesthesia system, Portable Anesthesia Machine (PAM, Summit Anesthesia Solutions, Bend, OR, USA, Part Number AS-01-0007) and a precision Tec 3 Isoflurane vaporizer pin (Summit Anesthesia Solutions, Part Number AA-00-1041-P) were used. The carrier gas was 100% oxygen supplied in E-tanks. The oxygen flow rate was set at 100 cc/min. The vaporizer was set at 1.0% isoflurane (Isothesia, Butler Animal Health Supply, Dublin, OH, USA) per volume of oxygen (7).

Regulation of ventilation for open chest imaging. According to our previously-developed procedure (7), to open the chest cavity, a 1-cm skin incision was made on the right side of the chest. The chest wall was opened without any injury to the lung. Then, an exhaust tube was half clamped to inflate the lung. This Positive End Expiratory Pressure (PEEP) system made it possible not only to keep the animal alive, but also to regulate lung inflation and deflation. By adjusting

the PEEP system to the appropriate pressure, the lungs were inflated to the proper fullness to optimally image cancer cells seeding the lung. The mouse was ventilated at the appropriate frequency by closing and opening the exhaust tube. After each observation period, the chest wall was closed with 6-0 sutures. During suturing, slight pressure was applied on the chest in order to reduce the volume of air in the chest cavity. The remaining air inside of the chest cavity was then suctioned in order to re-inflate the lung. The intubation tube was extubated when the mouse was breathing sufficiently. The mouse could be kept alive, and the same developing metastatic colonies could be observed at any time by reopening the chest wall with the techniques described above. Observations have been carried out for up to 8 h and repeated up to six times per mouse thus far (7).

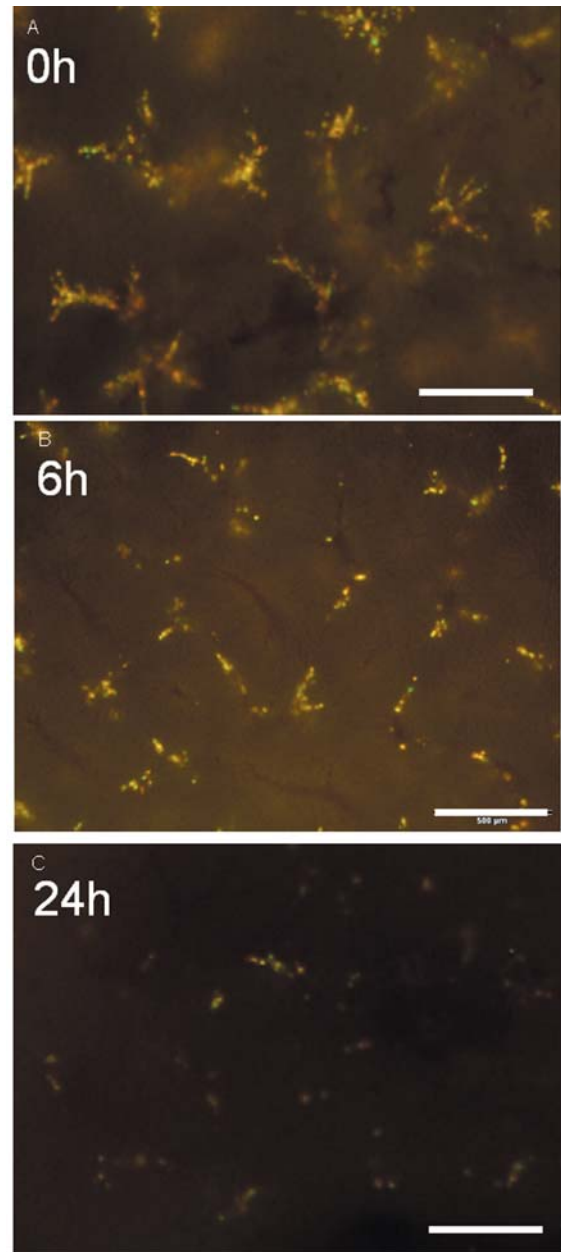
Imaging single cancer cell seeding in the lung. According to our previously-developed procedure (7), an intubated nude mouse was placed in an OV100 Small Animal Imaging System (Olympus Corp., Tokyo, Japan). A glass slide with clay stand was put on the



Lung

Figure 5. Time course of cancer cell survival after seeding in the lung. A: Dual-color HT-1080 cells seeding at 0 h. B: Surviving HT-1080 cells at 6 h. C: At 24 h, most of the HT-1080 cells had died or had been cleared out. Bars: A-C 200 μm .

lung to avoid excessive lung movement. This procedure is illustrated in Figure 1A-C. A total of 200 μl medium containing 10^6 dual-color HT-1080 cells was injected into the tail vein of the nude mice and imaging was immediately started. High-resolution images were captured directly on a PC (Fujitsu Siemens, Munich, Germany) as previously described (7).



Liver

Figure 6. Time course of cancer cell survival after seeding in the liver. A: At 0 hour. B: At 6 hours. C: At 24 hours. Bars: A-C 500 μm .

Cancer cell seeding in the liver and muscle. Four-week-old female nude mice were anesthetized with the ketamine mixture and laid on their back. For liver seeding, 10^6 dual-color HT-1080 cells were injected through a catheter in the portal vein of the mice during open laparotomy as previously described (9). A glass slide was put on the exteriorized liver of the mice to regulate motion. The mice

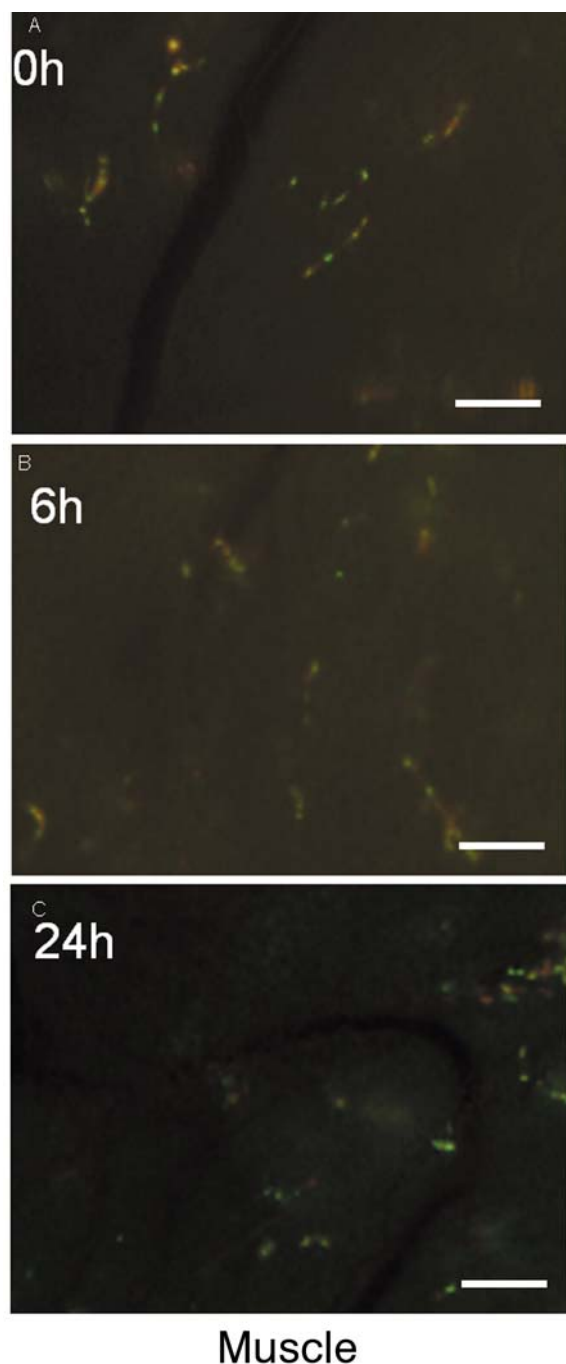


Figure 7. Time course of cancer cell survival after seeding in muscle. A: At 0 hour. B: At 6 hours. C: At 24 hours. Bars: A-C 200 μm .

were observed with the Olympus OV100 imaging system and images were taken, beginning immediately after cell injection.

For muscle seeding, 10^6 dual color HT-1080 cells were injected through a catheter into the abdominal aorta during open laparotomy. A glass slide was put on the exposed quadriceps muscle before observation with the OV100 imaging system. After imaging, the abdomen was closed and then reimaged at 24 h later with the same procedure.

Measurement of cancer cell deformation after seeding (6). Immediately after injection of the 10^6 dual-color HT-1080 cells into the tail vein, portal vein or abdominal aorta, deformation of the nuclei and cytoplasm of the cells was measured in the lung, liver and muscle. High magnification images of 20 randomly-selected cells were acquired. The axial length of the nuclei and cytoplasm were measured with OV100 software. Floating non-injected HT-1080 cells on a glass slide were also measured as controls. The experimental data were expressed as the mean \pm SD. Statistical analysis was carried out using the two-tailed Student's *t*-test.

Time course of cancer cell survival. Following the injection of 10^6 dual-color HT-1080 cells into the tail vein, portal vein or abdominal aorta of the nude mice, 30 fields ($550 \mu\text{m} \times 410 \mu\text{m}$) of the exposed lungs, liver or muscle were imaged at high magnification in each mouse at 0, 6 and 24 h with the OV100. After each time course observation, the chest wall or abdomen was closed with a 6-0 suture. The lung, liver or muscle was re-exposed for observation at 6 and 24 h. The total number of cells and number of dead cells (fragmented cytoplasm or nuclei) on the surface was counted. To determine whether immunoreactions were a factor in survival, HT-1080 cells were also injected into C57BL/6 mice for lung imaging. Cells were imaged in 4 immunocompetent and 4 nude mice. The experimental data are expressed as the mean of 4 mice, and the statistical difference between nude mice and immunocompetent mice was analyzed by Student's *t*-test.

Results

Subcellular imaging of cancer-cell seeding on the lung. Immediately after tail-vein injection, cancer cells arrested in the capillaries of the lung and many cells formed aggregates (Figure 2A-C). The distinction between live and dead cells was judged by nuclear and cytoplasmic integrity. After injection, some cells died by loss of cytoplasm or by fragmentation of cytoplasm and/or nuclei (Figure 2D-I).

Cancer-cell deformation in the lung, liver and muscle. In the lung and liver, little cell deformation occurred (Figure 3A and B). In contrast in the muscle, the dual-color HT-1080 cells were highly deformed (Figure 3C). The length of the cytoplasm of the HT-1080 cells was significantly different between muscle and the other organs or control (Figure 4A). The length of the nuclei of the HT-1080 cells was also significantly different between muscle and lung or control (Figure 4B).

Time course of cancer-cell survival after seeding in various organs. HT-1080 cell survival and the quantification of live and dead cells are shown in Figure 8. In the lung, a large number of cells arrested at 0 h, but the total cell number had decreased considerably at 6 and 24 hours. There was no significant difference between the nude mice and the immunocompetent C57BL/6 mice in cancer cell survival in the lung. The rate of cancer cell death was highest in the lung and lowest in the muscle. In each organ, single disseminated cells tended to die earlier than aggregated cells.

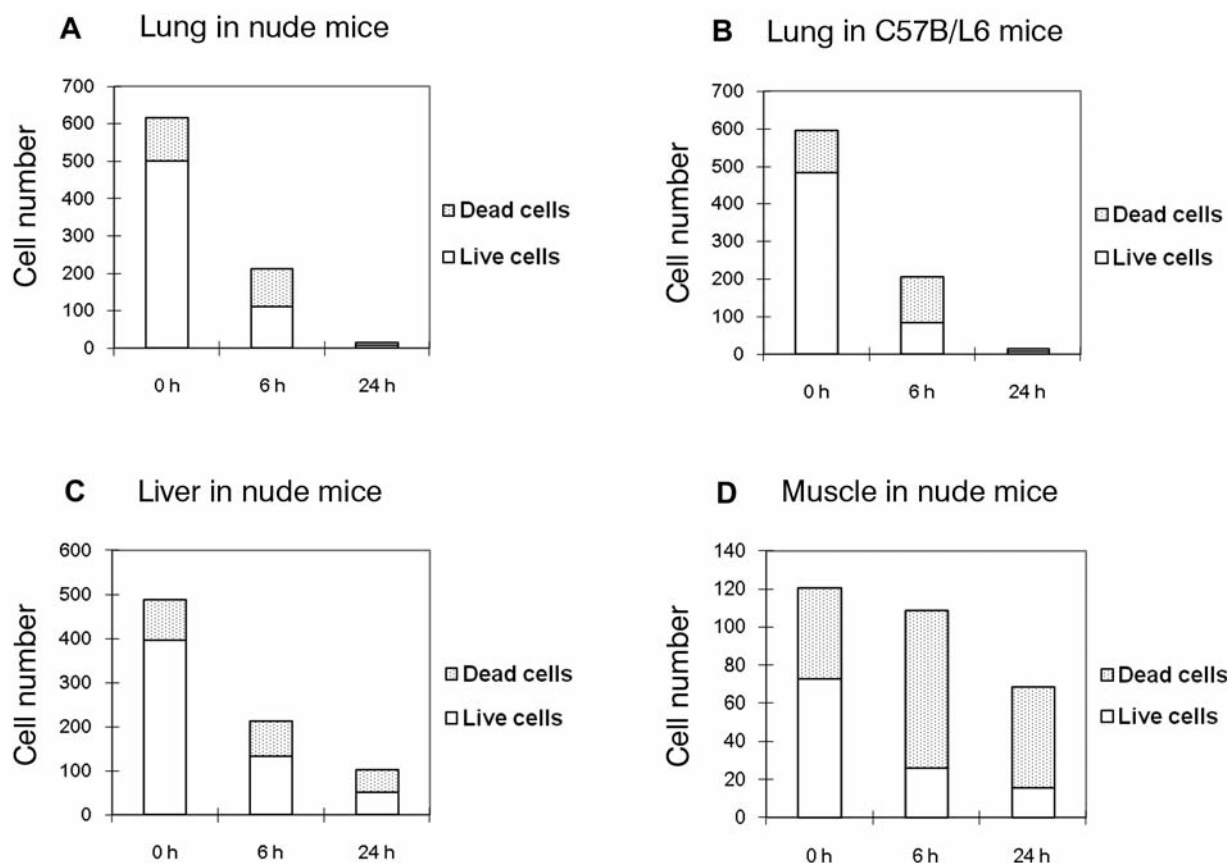


Figure 8. Quantification of live and dead cells in each organ. Cells in 30 high magnification fields were counted and expressed as an average of 4 mice.

Discussion

The behavior of the cancer cells after seeding was different in each organ. The cancer cells were highly stretched and often fragmented in the muscle, a high pressure microcirculation organ. In contrast, in the lung and liver, cancer cell deformation was minimal. The fate of the arrested cells was also different in each organ. In the lung, the cancer cells started to die immediately in contrast to slower cell death in the muscle and liver. Comparison of nude mice and immunocompetent mice, showed no significant difference in the rate of cell death within 24 hours, suggesting that T-cell reactions do not play an important role in the early steps of metastasis.

An important and early step during the formation of metastasis appears to be the arrest of tumor cells in the capillaries (10, 11). Two major hypotheses on the mechanisms of tumor cell arrest in metastatic host organs have been proposed. Ewing (12) hypothesized that random mechanical lodgment of circulating tumor cells in the first capillary system determined the location of secondary carcinomas. Paget (13) postulated in his “seed and soil” hypothesis that the successful

interaction of cancer cells (seeds) with the microenvironment of a particular target organ (soil) determines the formation of distant metastases in specific organs.

Some previous studies have described cancer cell seeding *in vivo*. When fibrosarcoma cells were injected into rat cremaster muscle (14), the majority of the cells passed quickly through the microcirculation and 88% of those that were arrested were destroyed over the course of the next hour. Weiss *et al.* (15) injected sarcoma cells into the mouse cremaster muscle and reported that most cells were mechanically trapped and deformed into cylindrical shapes in small capillaries and that the majority of these cells were rapidly destroyed within several minutes of injection. Morris *et al.* studied interactions of cancer cells with the microvasculature in muscle and liver with intravital microscopy (IVM) (16) and found that cells were arrested due to size restriction at the inflow side of the microvasculature and penetrated further and became more deformed in muscle than in liver. Schlüter *et al.* (17) investigated the relationship between the metastatic potential of colon carcinoma cells and their adhesive and invasive

behavior during early steps of metastasis within the microvasculatures of rat liver, lung, muscle and other organs. Their results indicated that the colon carcinoma cells could arrest in target organs without size restriction. Cell adhesion of circulating tumor cells occurred in metastatic target organs only and migration into target organs correlated with subsequent metastasis in that organ (17).

The present subcellular *in vivo* imaging study suggests that the early steps of metastasis are different in the lung, liver and muscle. The results in this report are important for the further understanding of metastasis and its effective treatment.

Acknowledgements

This study was supported in part by the National Cancer Institute grant CA132971.

References

- Chishima T, Miyagi Y, Wang X, Yamaoka H, Shimada H, Moossa AR and Hoffman RM: Cancer invasion and micrometastasis visualized in live tissue by green fluorescent protein expression. *Cancer Res* 57: 2042-2047, 1997.
- Yang M, Baranov E, Jiang P, Sun FX, Li XM, Li L, Hasegawa S, Bouvet M, Al-Tuwaijri M, Chishima T, Shimada H, Moossa AR, Penman S and Hoffman RM: Whole-body optical imaging of green fluorescent protein-expressing tumors and metastases. *Proc Natl Acad Sci USA* 97: 1206-1211, 2000.
- Hoffman RM: The multiple uses of fluorescent proteins to visualize cancer *in vivo*. *Nat Rev Cancer* 5: 796-806, 2005.
- Yamamoto N, Jiang P, Yang M, Xu M, Yamauchi K, Tsuchiya H, Tomita K, Wahl GM, Moossa AR and Hoffman RM: Cellular dynamics visualized in live cells *in vitro* and *in vivo* by differential dual-color nuclear-cytoplasmic fluorescent-protein expression. *Cancer Res* 64: 4251-4256, 2004.
- Yamauchi K, Yang M, Jiang P, Yamamoto N, Xu M, Amoh Y, Tsuji K, Bouvet M, Tsuchiya H, Tomita K, Moossa AR and Hoffman RM: Real-time *in vivo* dual-color imaging of intracapillary cancer cell and nucleus deformation and migration. *Cancer Res* 65: 4246-4252, 2005.
- Yamauchi K, Yang M, Jiang P, Xu M, Yamamoto N, Tsuchiya H, Tomita K, Moossa AR, Bouvet M and Hoffman RM: Development of real-time subcellular dynamic multicolor imaging of cancer-cell trafficking in live mice with a variable-magnification whole-mouse imaging system. *Cancer Res* 66: 4208-4214, 2006.
- Kimura H, Hayashi K, Yamauchi K, Yamamoto N, Tsuchiya H, Tomita K, Kishimoto H, Bouvet M and Hoffman RM: Real-time imaging of single cancer-cell dynamics of lung metastasis. *J Cell Biochem* 109: 58-64, 2010.
- Hoffman RM and Yang M: Subcellular imaging in the live mouse. *Nature Protocols* 1: 775-782, 2006.
- Tsuji K, Yamauchi K, Yang M, Jiang P, Bouvet M, Endo H, Kanai Y, Yamashita K, Moossa AR and Hoffman RM: Dual-color imaging of nuclear-cytoplasmic dynamics, viability, and proliferation of cancer cells in the portal vein area. *Cancer Res* 66: 303-306, 2006.
- Nicolson GL: Cancer metastasis: tumor cell and host properties important in colonization of specific secondary sites. *Biochim Biophys Acta* 948: 175-224, 1988.
- Feldman M and Eisenbach L: What makes a tumor cell metastatic? *Sci Am* 259: 60-65, 68, 85, 1988.
- Ewing J: A Treatise on Tumors, Neoplastic Diseases, ed 3. Philadelphia, Saunders, 1928.
- Paget S: The distribution of secondary growth in cancer of the breast. *Lancet* 133 (3421): 571-573, 1889.
- Blomqvist G, Skolnik G, Braide M, Bjursten L-M, Blixt A and Bagge U: Differences in lodgement of tumor cells in muscle and liver. *Clin Exp Metastasis* 6: 285-289, 1988.
- Weiss L, Nannmark U, Johansson BR and Bagge U: Lethal deformation of cancer cells in the microcirculation: a potential rate regulator of hematogenous metastasis. *Int J Cancer* 50: 103-107, 1992.
- Morris VL, MacDonald IC, Koop S, Schmidt EE, Chambers AF and Groom AC: Early interactions of cancer cells with the microvasculature in mouse liver and muscle during hematogenous metastasis: videomicroscopic analysis. *Clin Exp Metastasis* 11: 377-390, 1993.
- Schlüter K, Gassmann P, Enns A, Korb T, Hemping-Bovenkerk A, Hölzen J and Haier J: Organ-specific metastatic tumor cell adhesion and extravasation of colon carcinoma cells with different metastatic potential. *Am J Pathol* 169: 1064-1073, 2006.

Received April 22, 2011

Revised August 2, 2011

Accepted August 4, 2011